Supporting Information (SI)

SI Text:

1. The carbon-cycle model and the energy-balance model.

The model is an integrated carbon-cycle and one-box energy balance model. The carbon-cycle component adopts the Bern geochemistry model[1] to estimate atmospheric CO_2 and methane concentration from emissions. The radiative forcing due to GHGs is calculated from their atmospheric concentration, while the radiative forcing due to aerosols is scaled with emissions. The radiative forcing is then inputted into the energy balance model (similar to the formulation of ref. [2]) to calculate global mean temperature change. The model simulation compares well against observations of historical CO_2 concentrations (Fig. S1), temperature changes (Fig. 2), ocean heat content, and sea-level rise. The key parameters in the energy balance model are a 300-m ocean mixed layer and climate sensitivity of 0.8 (0.5 to 1.2 at the 10% to 90% confidence interval) $^oC/(W/m^2)$, or 3^{o}C due to a doubling of CO_2. And the probability density function of climate sensitivity is following the formulation in ref. [3], which is skewed more towards the high value of climate sensitivity ("fat tail", see more discussion in Section 4 (d) and Section 5 below). The probability density function of temperature projection is calculated by using 1500 randomizations at different values of climate sensitivity while keeping the forcing the same.

2. The scenarios.

Long-lived GHGs. In the Baseline-default scenario for CO_2, the emission keeps increasing throughout the 21st century (RCP8.5). The 5% to 95% range of baseline-default is also adopted (Fig. S1b). In the baseline-fast scenario for CO_2 (pre-INDCs), emissions effectively increase at a rate of 1.1%/year before 2030 and then following Representative Concentration Pathway 6.0 (Fig. S1a). In the mitigation scenario for CO_2 (i.e. INDCs and post-2030 decarbonization), emissions effectively increase at a rate of 0.8%/year before 2030 (following INDCs) and then decrease at a rate of 5.5%/year after 2030 (CN2030 in Fig. S2a). The CN2020 scenario is the same as CN2030, except that the peak of emission is reached at 2020 (Fig. S2b).

The other long-lived GHG with non-negligible forcing is nitrous oxide (N_2O). Its current forcing is approximately 0.15 W/m^2 and is projected to increase to 0.23 W/m^2 by 2100 (Fig. S6).

Net contribution to warming from 2010 to 2100 is only about 0.1ºC (50% probability). Given the small size of warming from present to 2100, and the fact that N_2O emission is tied to agriculture and thus has the greatest challenge in limiting N_2O emissions with a 10 billion population by 2100, we are not targeting N_2O in the following mitigation measures discussed here.

SLCPs. Under the baseline scenario, CH_4 emissions are projected to rise by 40% by 2030 from the 2005 level, and BC emissions are projected to increase by 15% by 2020 and then level off. The mitigation scenarios follow recommendations by the International Institute for Applied Systems Analysis (IIASA)[4] and the Royal Society[5] that maximum feasible reductions of air pollution regulations can result in reductions of 50% for CO emissions and 30% of CH_4 emissions from the 2005 levels by 2030, as well as reductions of 50% for BC emissions by 2050. The emissions of sulfates and their precursors are projected to decrease by 80% throughout the century. These aerosol scenarios are within the wide range suggested by a recent integrated-assessment model study[6], which included both "frozen legislation" (similar to our Baseline-fast) and "stringer legislation" (similar to our mitigation) scenarios. The total halocarbon forcing is slightly modified to include the Kigali Amendment to the Montreal Protocol that calls for a faster phase-out of HFC use[7]. The 2050 HFC forcing is projected to be about 10% of the 2020 value. Even under the stringent mitigation scenario, a residual radiative forcing of HFC that is higher than the 2000 level (about 0.05 W/m^2) is included[8].

The time series of total radiative forcing applied to the energy balance model are given in Fig. S4 and the radiative forcing due to individual compositions are given in Fig. S6. We note that CH_4 effects include forcing through the formation of tropospheric O_3 and stratospheric water vapor. BC effects also factored in co-emitted organic carbon, which partially offset the warming effects. Thus, the industrial era climate forcing (present-day minus 1850) of BC forcing in this paper is 0.7 W/m^2, a conservative value compared to the 1.1 W/m^2 in a recent assessment[9].

SLCP mitigation requires a multi-dimensional and multi-sectoral approach[10]. (a) In the case of HFCs, mitigation requires coordination with the Montreal Protocol since HFCs are proposed to be covered by an amendment to this treaty[11]. (b) BC is a major air pollutant. In urban areas, BC emissions from diesel vehicles are a primary source of particulate matter. Emissions of BC and organic aerosols by biomass cook stoves are the principal air pollutants in rural areas and are responsible for nearly three million deaths worldwide[12]. (c) CH_4 is a GHG itself but also leads to the production of tropospheric ozone, which is a GHG as well as a major air pollutant with negative impacts on public health and crop yields. BC and methane mitigation require coordination with urban and national air pollution agencies. A good example is the recent California Air Resource Board initiative on SLCPs[13]. The combustion of coal and petroleum release sulfur dioxide (SO_2), which is converted to sulfate particles. These sulfates reflect sunlight, which results in cooling. The cooling effect of co-emitted sulfate and nitrate particles has masked as much as 30-50% of the warming effect of CO_2 released by fossil fuels. SO_2 and NO_x emissions are eliminated when energy sources are switched from fossil fuels to renewables and the warming produced by the unmasking of sulfate/nitrate effects during the coming decades partially offsets the cooling effect of CO_2 mitigation[14], [15]. The co-benefit of taking explicit measures of mitigating SLCP emissions is immense. Nearly seven million people die every year due to ambient air pollution, to which sulfates and nitrates contribute as much 40%. Likewise, some of the warming effects of black carbon emissions are offset by the cooling effect of organics aerosols; however, reducing organic aerosols along with black carbon resulting from biomass cooking and other sources can save millions of lives every year.

The use of carbon extraction and sequestration (CES) is a promising avenue being pursued by many groups[16] with applications for power, heat, and transportation fuels. Biomass, depending on the source and harvesting practices, is a carbon neutral energy source for production of bioenergy[17]. Capture of CO_2 can be accomplished in bioenergy power plants, biochar production by pyrolysis and storage in soils, and restoration of soil organic pools. Our analysis suggests that urgent investments in these avenues are needed so that scalable technology will be available by 2030. Such a window is closing quickly[18].

3. Validation of the climate sensitivity: equilibrium and transient values.

The central value (50% probability) of the equilibrium climate sensitivity of the model is 3.0ºC for a doubling of carbon dioxide. The climate models used in the IPCC studies have been calibrated by comparing two metrics. First is the equilibrium climate warming due to a doubling of carbon dioxide concentration and this warming is referred as equilibrium climate sensitivity (ECS). The second important metric is the transient climate response (TCR). This is estimated by increasing the CO_2 concentration by 1% each year until it doubles at year 70. The simulated warming for the year when CO_2 doubles is the TCR. The most recent IPCC report compared ECS and TCR for 30 models from around the world[19]. The 30-model mean for ECS is 3.2ºC (2.1ºC to

4.7ºC for the minimum to maximum range), compared well with the 3.0ºC for the model used in this study. The ECS comparison suggests that the treatment of the net effects of climate physical-dynamical feedback processes in the model used in this study is consistent with the more comprehensive three-dimensional climate models used in IPCC assessment report. With respect to TCR, which is a crucial test for the treatment of ocean thermal inertia, the 30-model mean is 1.8ºC (minimum to maximum range of 1.1ºC to 2.6ºC), which again compares favorably with the TCR of 1.8ºC for the present model. The ECS and TCR are hotly debated issues and many studies have attempted to infer it from observed temperature and forcing trends for the 20^{th} century. Few of these studies[20, 21] obtained ECS or TCR values that are about 50% smaller than the IPCC multi-model mean. A more recent study that corrects for sampling errors in observational trends, obtained a TCR of 1.7ºC[22], again consistent with the 1.8ºC value used in this study.

4. Uncertainties treatment in the modeled warming.

We have included the following sources of uncertainties into consideration:

(a) Emission scenarios These arise in projecting population growth, carbon intensity of energy, carbon intensity of the economy, the growth of GDP and consumption patterns among others. And we have adopted both Baseline-fast and Baseline-default scenarios (Fig. 1 and Fig. 2) as well as the 5%-95% associated with each scenario (Fig. S1).

(b) Modeling of aerosol and cloud processes (Fig. 1). Aerosol forcing is a major source of uncertainty in calculating the historical radiative forcing, and the spread in the aerosol forcing for the year 2010, can range from 0 to −2 Wm^{-2}[23]. In exploring the role of this uncertainty, we account for the entanglement of the aerosol forcing uncertainty with climate sensitivity uncertainty (blue dashed line in Fig. 1). That is, if a higher climate sensitivity is used, the historical aerosol forcing needs to be more negative to simulate the observed temperature trends of the 20^{th} century. For each climate sensitivity value selected, we adjust the historical aerosol forcing (but staying within the 0 to −2 Wm^{-2} range) to obtain the optimal fit for the 20th-century temperature trends, and then apply the same adjustment for the future aerosol forcing. Because of the mutually compensating effect of the aerosol forcing with climate sensitivity (more negative aerosol forcing requires larger climate sensitivity to explain the observed warming), the aerosol forcing uncertainty turns out to have a smaller effect than expected on the spread of the 2100 warming (Fig. 1 of ref[24]).

(c) Carbon-cycle climate feedbacks. There are three positive feedbacks identified so far: decrease in oceanic and land uptake of the emitted carbon which amplifies the increase in atmospheric CO_2; thawing of permafrost which releases CO_2 and CH_4 to the atmosphere; and increased emission of CH_4 from the warmer wetlands. Most of the climate models do not include the CO_2 and CH_4 released by the permafrost or the wetlands. These positive feedbacks are effectively considered in Fig. 1.

(d) Physical-dynamical climate feedbacks. The largest source of climate sensitivity uncertainty is that due to the physical-dynamical feedbacks arising from water vapor (the largest greenhouse gas), clouds (the dominant regulator of radiative forcing), and snow/ice albedo from melting of Arctic sea ice and glaciers among other parts of the cryosphere.

5. Origin of the skewed distribution of climate sensitivity.

We adopted the skewed distribution of climate sensitivity derived by Roe and Baker [3].This distribution was derived from the several tens of published studies with three-dimensional climate models (3), yielding a central value of 3ºC warming for a doubling of CO_2 (definition for climate sensitivity) with a 95% range of 2ºC to 4.5ºC[25]. The distribution is asymmetric (skewed) with a well-defined lower bound but without a sharp upper bound. To examine if this is reasonable, let us consider the 1% probability value for the distribution adopted for Fig. 1, which is about 5.5ºC for a doubling of CO_2, compared with the central value of 3ºC. Is the 5.5ºC climate sensitivity reasonable or unrealistically high? A recent 3-D coupled ocean-atmosphere climate model study[26] showed that when the model included the mixed ice-water phase clouds, the climate sensitivity increased from 4ºC to 5.3ºC. Global climate models assessed by ref (3) included the ice/snow albedo feedback, but a recent study[27] using satellite data showed the observed ice/snow albedo decreased more steeply with warming than that depicted in models. Also, satellite data showeda large retreat of the mid-latitude storm track clouds with warming than that revealed by model studies[28]. Since these cloud systems have a large radiative cooling effect (because of their albedo), underestimation of their poleward retreat will underestimate their positive feedback effect. The basic inference is that the 1% probability of 5.5ºC climate sensitivity in the ref 3 distribution can not be ruled out as out of bounds of likely values.

6. Individual contributions to mitigation.

With unchecked emissions, the warming can become as large as 5.0ºC (baseline-default. Fig. 1). Just reducing the carbon intensity of the economy from the projected 50% (from 2010 values) by 2100 (under baseline-default) to 80% (under baseline-fast), will cut CO_2 concentration sufficiently to reduce the warming by 0.9ºC. Reducing CO_2 by achieving carbon neutrality will reduce the warming by at least another 1.6ºC to 1.9ºC (Table S1). However, the 0.6ºC warming caused by unmasking of aerosol cooling (most of which is due to fossil fuels) would offset some of the cooling due to CO_2 mitigation. What fraction of this unmasking is caused by CN measures versus air pollution regulations would depend on the relative timing of CN measures and air pollution regulations. Reducing the super pollutant emissions through a combination of CO_2 and SLCP measures, can reduce the warming by another 1.2ºC. Extracting one trillion tons of CO_2 from the air would cut the warming by another 0.3ºC by 2100 and therefore achieve WB2C goal and also bend the warming curve to a cooling trend (Fig. 3).

SI Table:

Table S1. The contribution of individual mitigation measures to the warming in the 21st century.

Mitigation Measure	2050 change in ºC	2100 change in ºC	Estimated in
Energy Intensity	−0.2	−0.9	Fig. 1, Fig. S1
CO_2 due to CN2030	−0.1	−1.6	Fig. S3
CO_2 due to CN2020	−0.3	−1.9	Fig. 3
CO_2 due to CES1t	0	−0.3	Fig. S3
BC	−0.2	−0.3	Fig. S3, Fig. S6
CH_4 including O_3	−0.2	−0.45	Fig. S3, Fig. S6
HFCs	−0.2	−0.45	Fig. S3, Fig. S6
Aerosol Unmasking	+0.3	+0.6	Fig. S7

SI Figures:

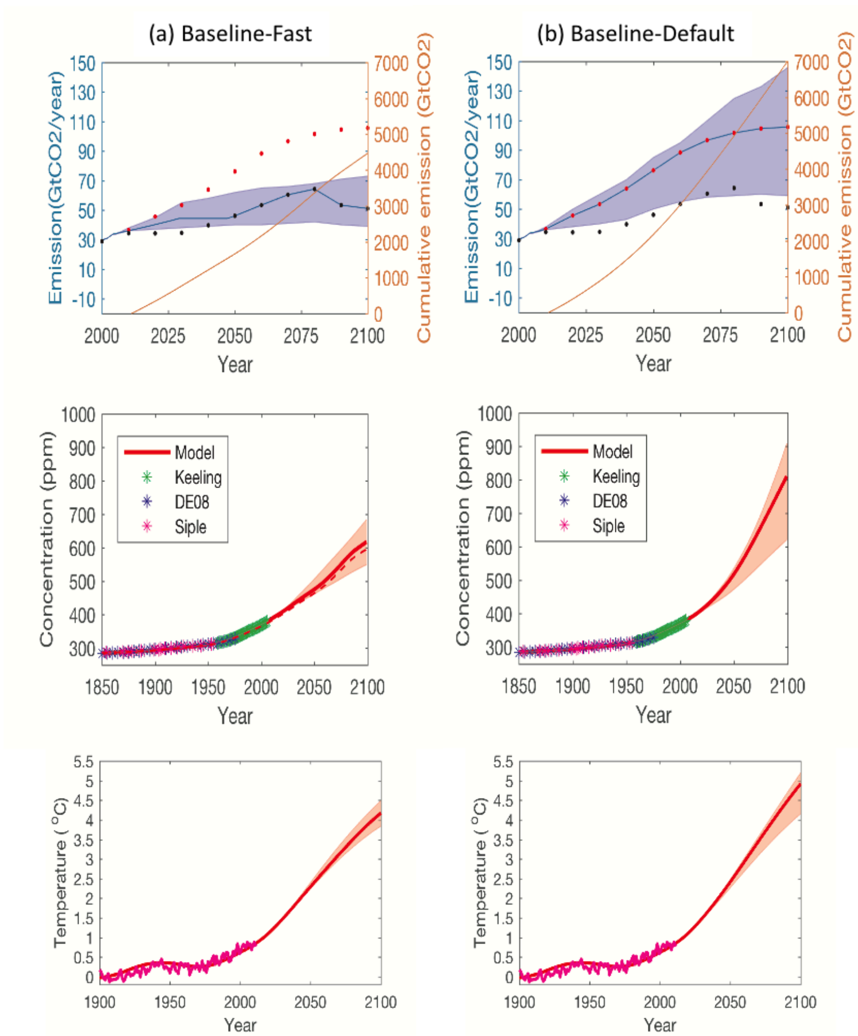

Fig. S1. (a) Under the Baseline-fast scenario. CO_2 emission rate (blue curve, Gt CO_2/year), CO_2 cumulative emissions since 2010 (red curve, Gt CO_2) are shown in the upper panel. The 5% to 95% uncertainty of the emission pathway (as adopted from Figure 6.4 of ref [29]) is also shown in the shading. CO_2 emission in RCP8.5 (red dots) and RCP6.0 (black dots) are shown for comparisons. In the middle panel, simulated CO_2 atmospheric concentration (red curve, ppm) is shown along with the 5% to 95% uncertainty range. The red dashed line is the simulated CO_2 concentration when the land carbon uptake coefficient in the carbon cycle model is increased by 20%. In the bottom panel, simulated temperature increase (red curve, ºC) in shown along with the

5% to 95% uncertainty due to CO_2 pathway, not due to climate sensitivity. (b) Same as (a), except for the baseline-default scenario[29], which is more in line with RCP8.5.

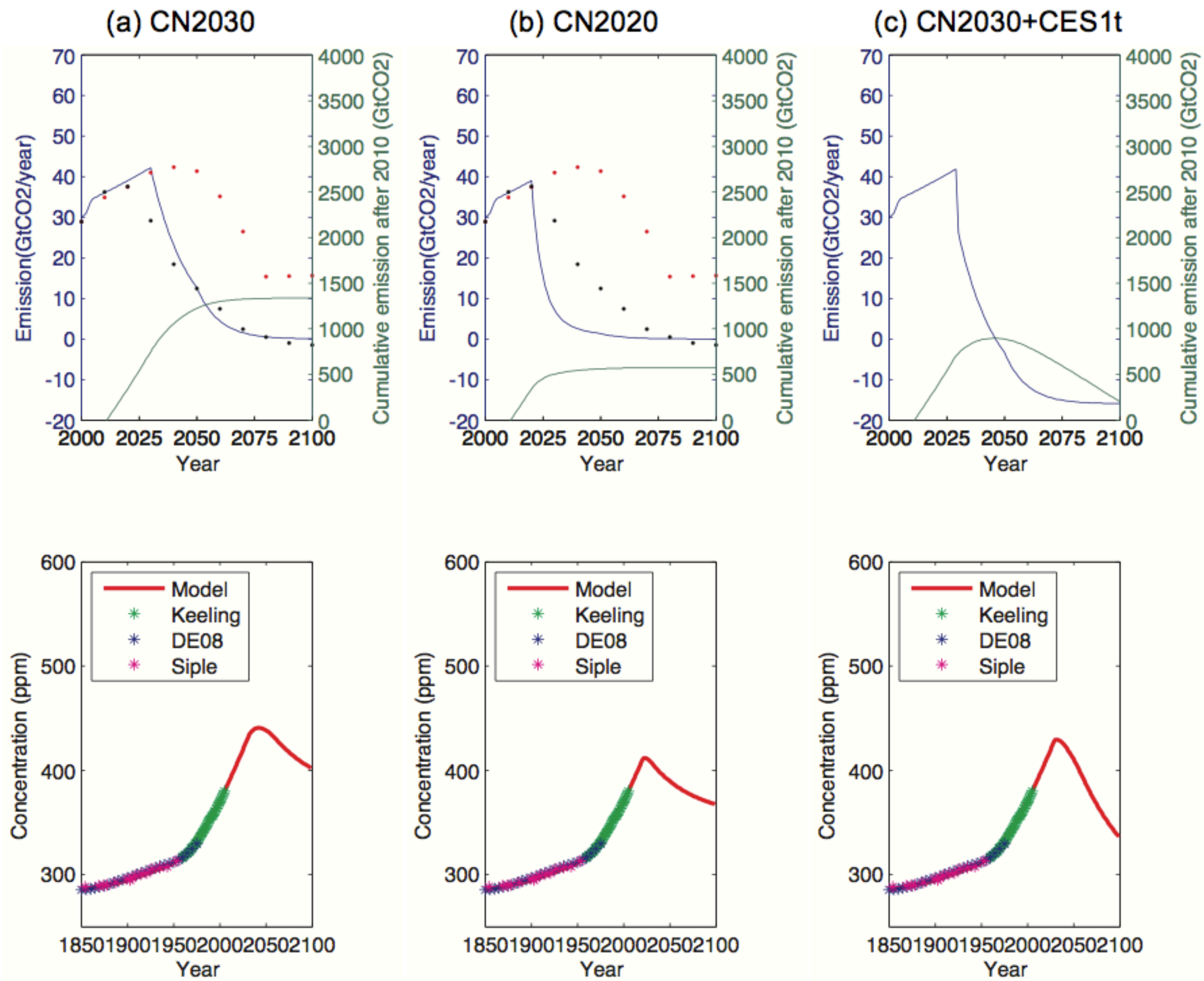

Fig. S2. (a) CO_2 emission rate (blue curve in the upper panel, Gt CO_2/year), CO_2 cumulative emissions since 2010 (green curve in the upper panel, Gt CO_2) and CO_2 atmospheric concentration (red curve in the lower panel, ppm) under the CN2030 scenario (CO_2 mitigation starting from 2030, which follows the INDCs before 2030 and then a post-2030 decarbonization pathway). CN is eventually reached at about 2060-2070. CO_2 emission in RCP4.5 (red dots) and RCP2.6 (black dots) are shown for references. Simulated historical CO_2 concentration is consistent with various observational records since the 1850s (color dots in the lower panel). (b) Same as (a), except that the CO_2 mitigation starts earlier at 2020 (CN2020). CN is reached at about 2040-2050. (c) Same as (a) with CO_2 mitigation starting at 2030, but also including an additional carbon extraction and sequestration (CES) at a rate of 16 Gt CO_2/year after 2030.

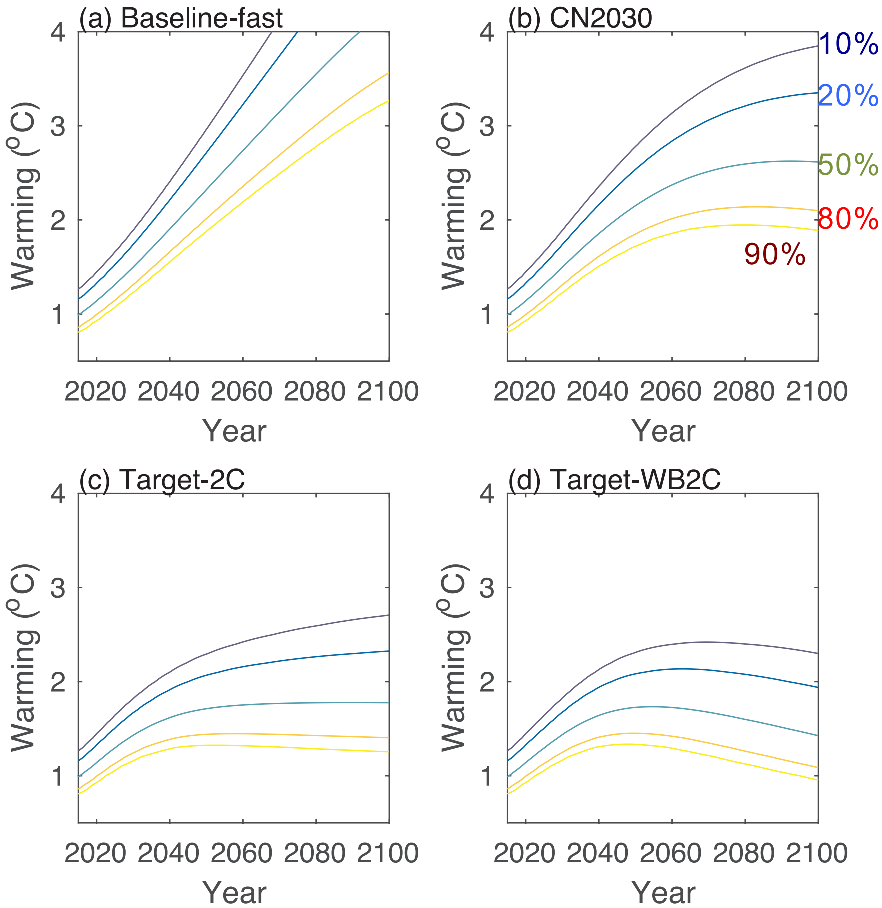

Fig. S3. The probability of exceeding a certain temperature threshold (Y-axis) at a given year (X-axis) under different scenarios. (a) Baseline-fast. (b) CO_2 mitigation only (CN2030). (c) CO_2 mitigation + SLCP mitigation (CN2030+SLCP2020, Target-2C). (d) CO_2 mitigation + SLCP mitigation + CES at a rate of 16 Gt CO_2/year (CN2030+SLCP2020+CES1t, Target-WB2C).

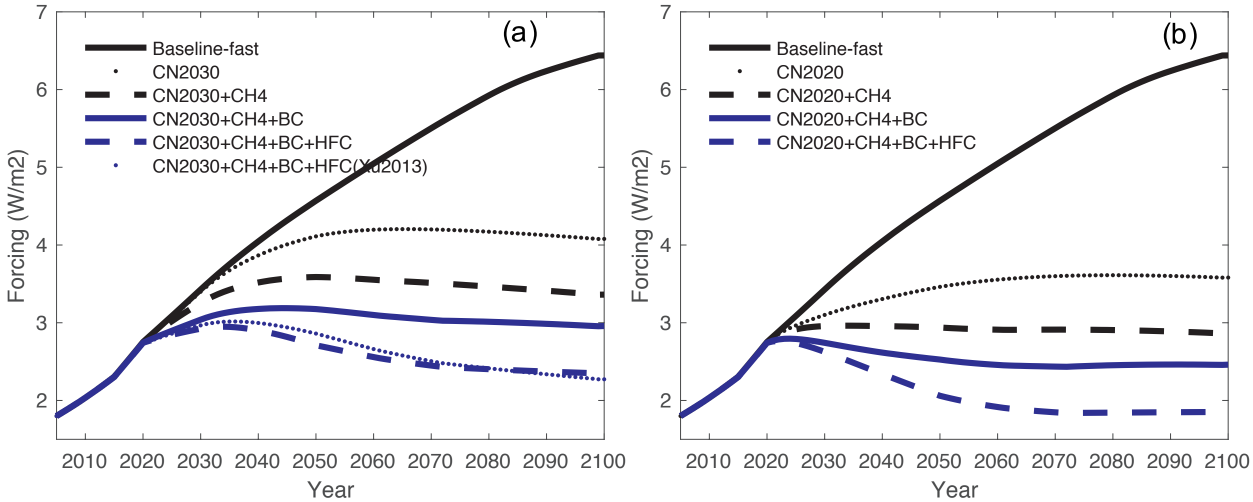

Fig. S4. (a) 21st century radiative forcing due to a combination of CO_2 and SLCP mitigation (Target-2C: CN2030+SLCP2020). Note: the blue dots represent the HFC scenario used in a previous study (30). (b) Same as (a) but for Target-1.5C (CN2020+SLCP2020).

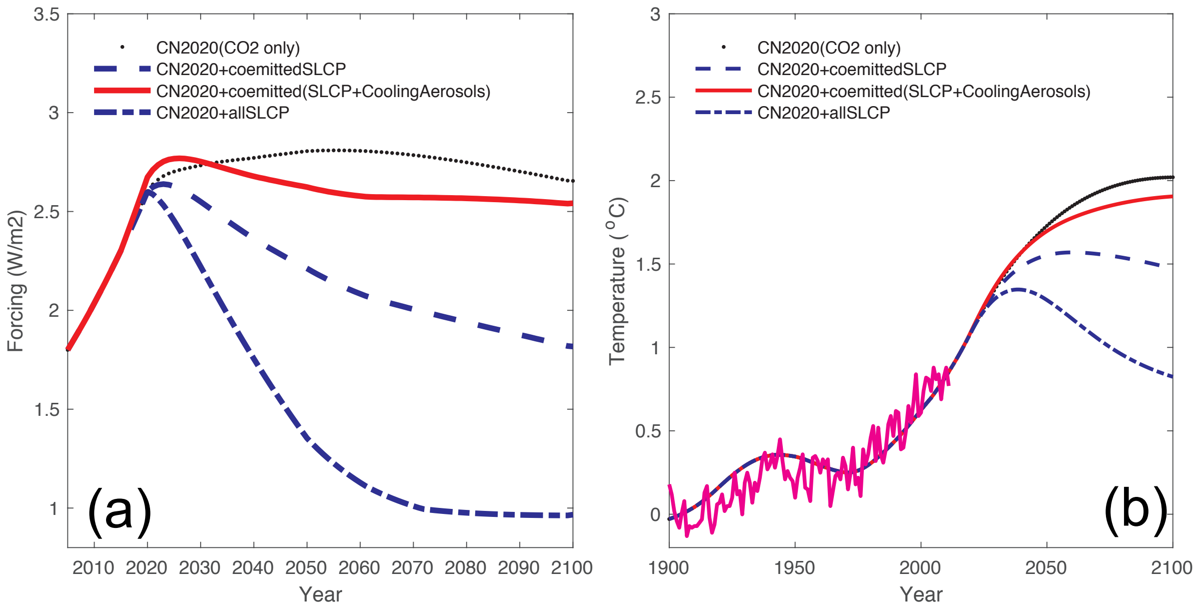

Fig. S5. The role of co-emitted SLCPs and cooling aerosols with CO_2 in the CN2020 measures. (a) Black line is the radiative forcing due to CO_2 mitigation only resulting from the CN2020 measures (note that the SO_4 and nitrate cooling is fixed in this case, so it is not directly comparable with the CN2020 curves in Fig. S4b), and the blue dashed line down below shows the mitigation of CH_4 and BC emissions co-emitted with CO_2 sources, which lowers the radiative forcing by 0.8 W/m^2 at 2100. The dashed-dotted line includes the mitigation of all SLCPs by dedicated SLCPs measures. By comparing the difference between three lines, we can estimate the fraction of the SLCPs mitigation that can be accomplished by the CO_2-dedicated measures, and the fraction that can only be accomplished by the SLCPs-dedicated measures. The red line includes the mitigation of co-emitted sulfate and nitrate aerosols, in addition to the co-emitted SLCPs with CO_2, which tends to warm the atmosphere. (b) Same as (a), but for the temperature projection under various scenarios.

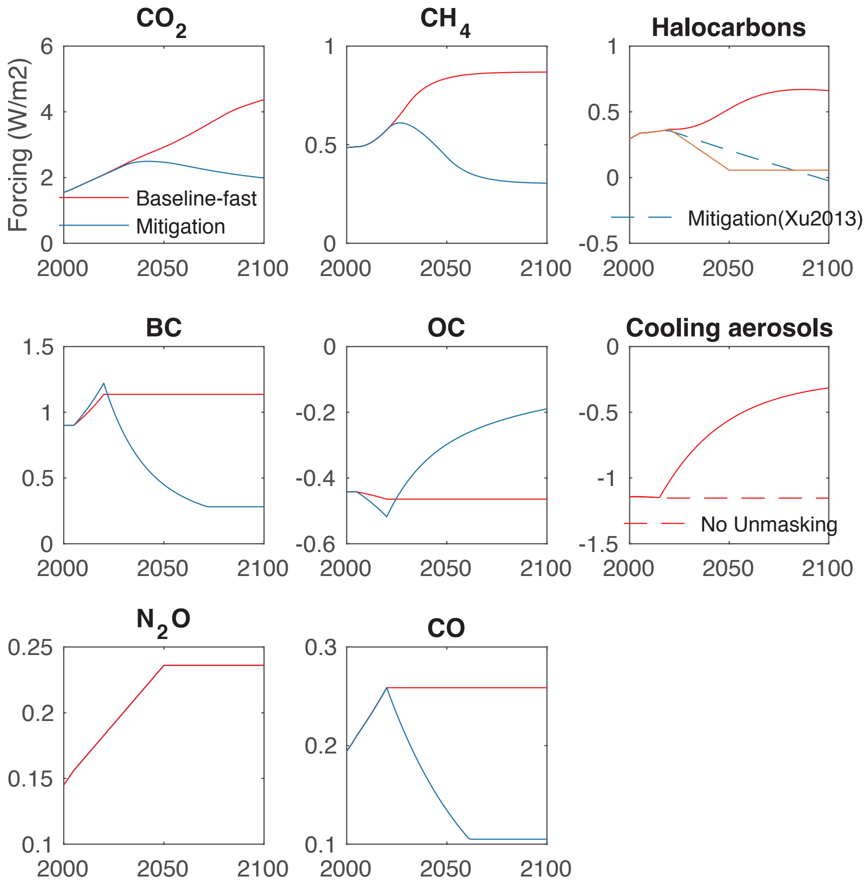

Fig. S6. Radiative forcing (W/m^2) due to individual atmospheric compositions under the baseline (red) and mitigation (blue) scenarios. The CO_2 baseline here is the Baseline-fast scenario and the mitigation scenario here refers to CN2030. The "cooling aerosols" panel shows the cooling aerosol forcing (due to sulfates, nitrates, and indirect effects through clouds) under baseline scenario (reduction in red solid line) and "No Unmasking" scenario (flat red dashed line). The upper right panel also shows the halocarbon scenario used in our previous study[30].

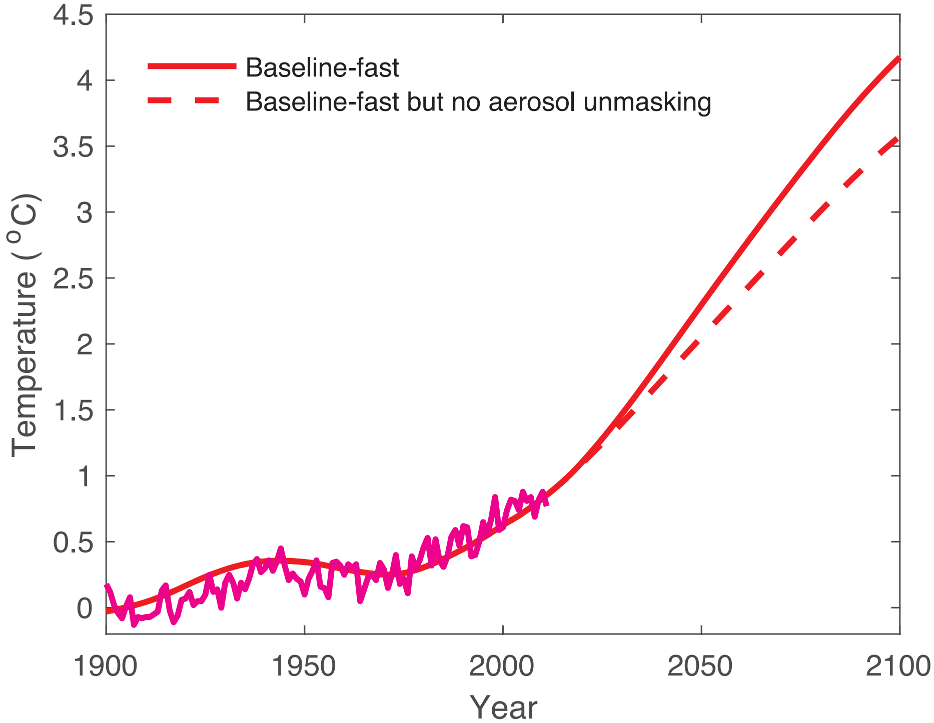

Fig. S7. The warming under Baseline-fast scenario (red solid line) is the same as in Fig. 3. The red dashed line also shows the warming under Baseline-fast scenarios but without unmasking of cooling aerosols, Fig. S6). The additional warming due to the unmasking of cooling aerosols (as the difference between red solid and red dashed lines) is 0.25ºC at 2050 and 0.6ºC at 2100.

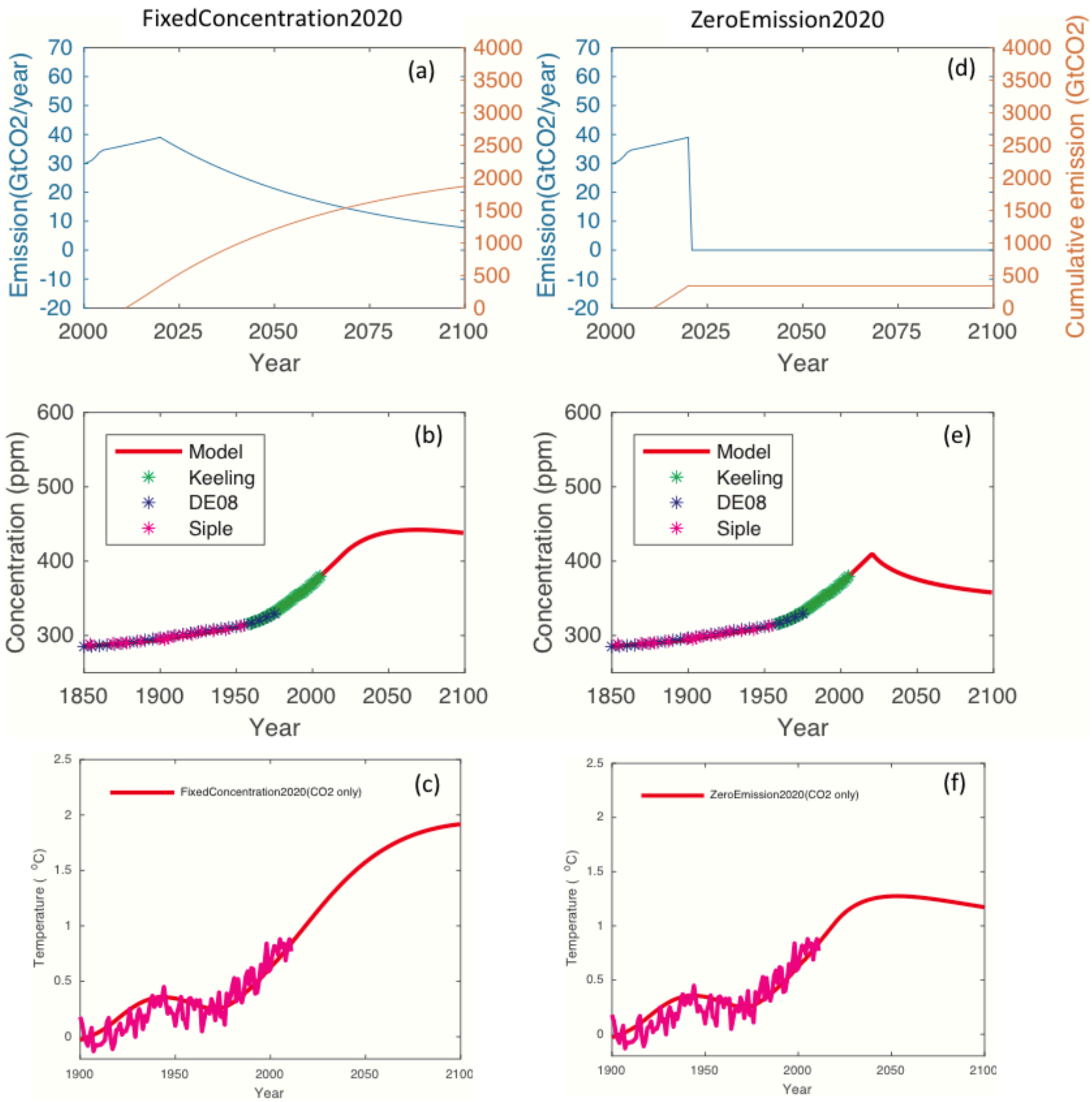

Fig. S8. (a) A "Fixed Concentration" scenario for CO_2 that is similar to Fig. S2b (CN2020), except that the decarbonization pathway is slower and the carbon neutralization (CN) is not reached until the end of the century. (b) Due to the slower pathway to reach CN, the CO_2 concentration levels off at 2020-2030 values ("Fixed Concentration") instead of declining as in Fig. S2b (CN2020). (c) The temperature simulated under FixedCocentration2020 (due to CO_2 forcing only, with SLCP and cooling aerosol forcing fixed at present-day level) is shown in red. (d), (e), (f): Similar to (a), (b), (c), except under a scenario in which the CO_2 emission becomes to net zero after 2020 ("ZeroEmission2020"). Because of the thermal inertia of the oceans, there is an unrealized warming of about 0.6ºC due to cumulative emissions as of 2030. If the emissions of CO_2 were reduced to zero immediately (d), CO_2 concentrations would decrease (e). Focusing just on CO_2, the resulting decrease in radiative forcing can either offset or exceed the heat stored in the oceans such that the CO_2 warming can stabilize at 2030 levels or even decrease slightly (f).

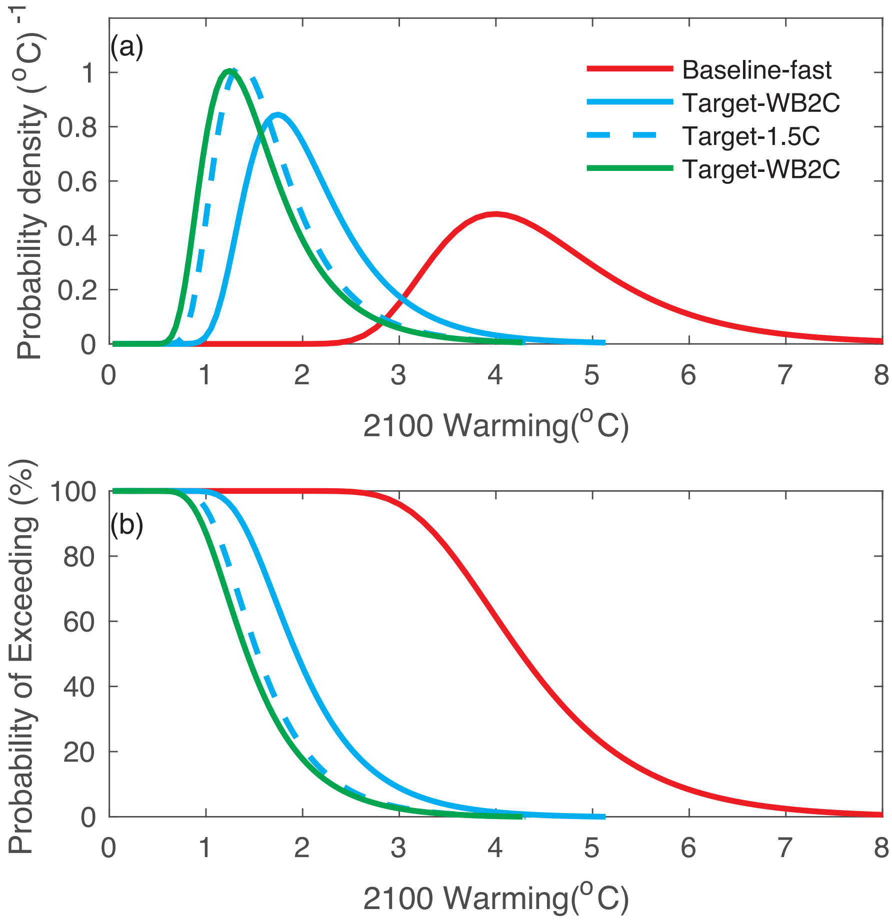

Fig. S9. (a) Similar to Fig. 2, but also showing two additional scenarios: CN2030+SCLP2020 (Target-2C) in blue solid line and CN2020+SLCP2020 (Target-1.5C) in blue dashed line. (b) The probability of exceeding a certain temperature threshold (X-axis) in 2100, calculated as 1- the cumulative distribution function of the curves in (a).

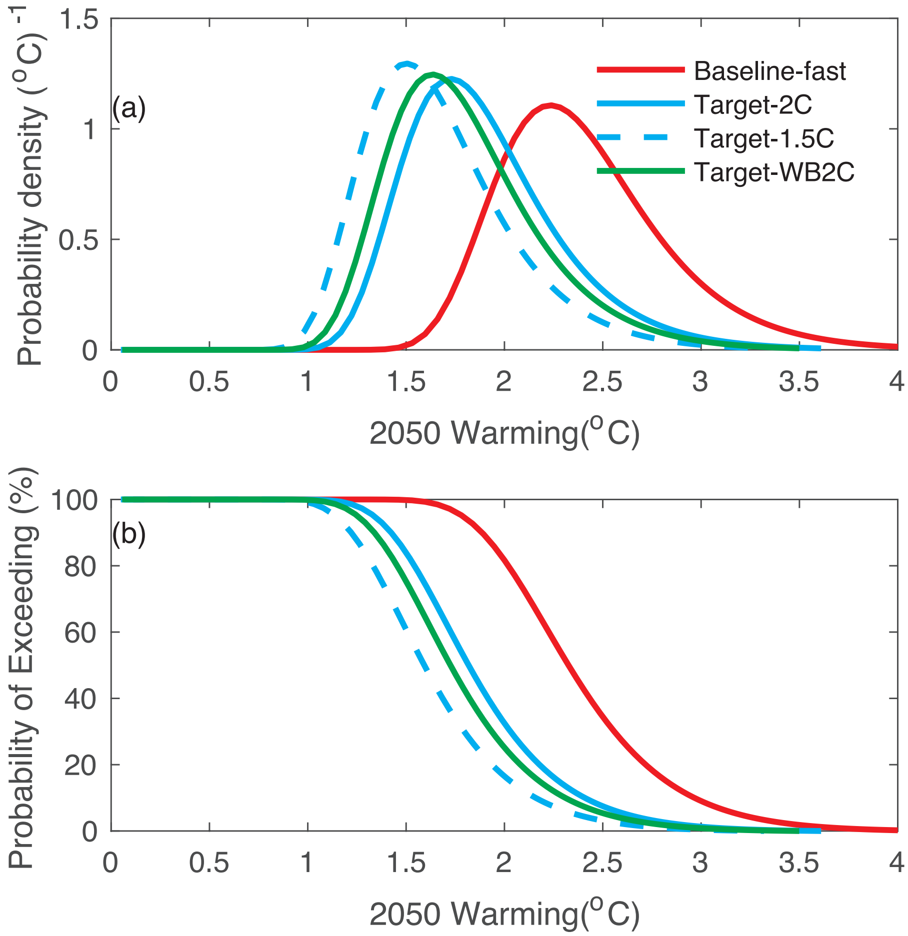

Fig. S10. Same as Fig. S9, but for 2050.

SI References

1 Joos F, et al. (1996) An efficient and accurate representation of complex oceanic and biospheric models of anthropogenic carbon uptake. Tellus, Ser B Chem Phys Meteorol 48(3):397–417. Available at: http://dx.doi.org/10.1034/j.1600-0889.1996.t01-2-00006.x.

2 Held IM, et al. (2010) Probing the fast and slow components of global warming by returning abruptly to preindustrial forcing. J Clim 23(9):2418–2427. Available at: http://dx.doi.org/10.1175/2009JCLI3466.1.

3 Roe GH, Baker MB (2007) Why Is Climate Sensitivity So Unpredictable? Science (80-) 318(5850):629–632. Available at: http://www.sciencemag.org/content/318/5850/629.

4 Cofala J, Amann M, Klimont Z, Kupiainen K, Höglund-Isaksson L (2007) Scenarios of global anthropogenic emissions of air pollutants and methane until 2030. Atmos Environ 41(38):8486–8499.

5 Royal Society (2008) Ground-level ozone in the 21st century: Future trends, impacts and policy implications. http://royalsociety.org/displaypagedoc. asp?id=31506.

6 Rogelj J, et al. (2014) Air pollution emission ranges consistent with the representative concentration pathways. Nat Clim Chang 4(May):1–5. Available at: http://www.nature.com/doifinder/10.1038/nclimate2178.

7 http://www.unep.org/ozonaction/Portals/105/documents/7809-e-Factsheet_Kigali_Amendment_to_MP.pdf

8 Velders GJM, Fahey DW, Daniel JS, Andersen SO, McFarland M (2015) Future atmospheric abundances and climate forcings from scenarios of global and regional hydrofluorocarbon (HFC) emissions. Atmos Environ 123:200–209. Available at: http://www.sciencedirect.com/science/article/pii/S135223101530488X.

9 Bond TC, et al. (2013) Bounding the role of black carbon in the climate system: A scientific assessment. J Geophys Res Atmos 118(11):5380–5552.

10 Wallack J, Ramanathan V (2009) The Other Climate Changes, Why Black Carbon Also Matters, Foreign Affairs, Sept/Oct 2009, pp. 105-113.

11 Molina M, et al. (2009) Reducing abrupt climate change risk using the Montreal Protocol and other regulatory actions to complement cuts in CO2 emissions. Proc Natl Acad Sci U S A 106(49):20616–20621.

12 Lim SS, et al. (2012) A comparative risk assessment of burden of disease and injury attributable to 67 risk factors and risk factor clusters in 21 regions, 1990-2010: A systematic analysis for the Global Burden of Disease Study 2010. Lancet 380(9859):2224–2260. Available at: http://dx.doi.org/10.1016/S0140-6736(12)61766-8.

13 CARB. (2015) Short-Lived Climate Pollutant Reduction Strategy. http://www.arb.ca.gov/cc/shortlived/2015draft.pdf

14 Brasseur GP, Roeckner E (2005) Impact of improved air quality on the future evolution of climate. Geophys Res Lett 32(23): L23704. Available at: http://dx.doi.org/10.1029/2005GL023902.

15 Xu Y, Lamarque JF, Sanderson BM (2015) The importance of aerosol scenarios in projections of future heat extremes. Clim Change:1–14. Available at: http://dx.doi.org/10.1007/s10584-015-1565-1.

16 NRC (2015). Climate Intervention: Carbon Dioxide Removal and Reliable Sequestration. http://www.nap.edu/catalog/18805/climate-intervention-carbon-dioxide-removal-and-reliable-sequestration

17 Ragauskas AJ, et al. (2006) The Path Forward for Biofuels and Biomaterials. Science (80-) 311(5760):484–489. Available at: http://science.sciencemag.org/content/311/5760/484.abstract.

18 Scott V, Gilfillan S, Markusson N, Chalmers H, Haszeldine RS (2012) Last chance for carbon capture and storage. Nat Clim Chang 3(2):105–111. Available at: http://dx.doi.org/10.1038/nclimate1695.

19 Flato G, et al. (2013): Evaluation of Climate Models. In: Climate Change 2013: The Physical Science Basis. Contribution of Working Group I to the Fifth Assessment Report of the Intergovernmental Panel on Climate Change [Stocker, T.F., D. Qin, G.-K. Plattner, M. Tignor, S.K. Allen, J. Boschung, A. Nauels, Y. Xia, V. Bex and P.M. Midgley (eds.)]. Cambridge University Press, Cambridge, United Kingdom and New York, NY, USA.

20 Skeie RB, Berntsen T, Aldrin M, Holden M, Myhre G (2014) A lower and more constrained estimate of climate sensitivity using updated observations and detailed radiative forcing time series. Earth Syst Dyn:139–175.

21 Stott P, et al. (2013) The upper end of climate model temperature projections is inconsistent with past warming. Environ Res Lett 8(1):14024. Available at: http://stacks.iop.org/1748-9326/8/i=1/a=014024.

22 Richardson M, Cowtan K, Hawkins E, Stolpe MB (2016) Reconciled climate response estimates from climate models and the energy budget of Earth. Nat Clim Chang (June):1–6.

23 Myhre G (2013) Anthropogenic and Natural Radiative Forcing. In: Climate Change 2013: The Physical Science Basis. Contribution of Working Group I to the Fifth Assessment Report of the Intergovernmental Panel on Climate Change [Stocker, T.F., D. Qin, G.-K. Plattner, M. Tignor, S.K. Allen, J. Boschung, A. Nauels, Y. Xia, V. Bex and P.M. Midgley (eds.)]. Cambridge University Press, Cambridge, United Kingdom and New York, NY, USA.

24 Meinshausen M, et al. (2009) Greenhouse-gas emission targets for limiting global warming to 2ºC. Nature 458(7242):1158–1162. Available at: http://dx.doi.org/10.1038/nature08017.

25 Stocker TF, et al. (2013) Technical Summary. In: Climate Change 2013: The Physical Science Basis. Contribution of Working Group I to the Fifth Assessment Report of the Intergovernmental Panel on Climate Change [Stocker, T.F., D. Qin, G.-K. Plattner, M. Tignor, S.K. Allen, J. Boschung, A. Nauels, Y. Xia, V. Bex and P.M. Midgley (eds.)]. Cambridge University Press, Cambridge, United Kingdom and New York, NY, USA

26 Tan I, Storelvmo T, Zelinka MD (2016) Observational constraints on mixed-phase clouds imply higher climate sensitivity, Science, 352, 6282, 224-227, doi: 10.1126/science.aad5300

27 Pistone K, Eisenman I, Ramanathan V (2014) Observational determination of albedo decrease caused by vanishing Arctic sea ice. Proc Natl Acad Sci 111(9):3322–3326. Available at: http://www.pnas.org/lookup/doi/10.1073/pnas.1318201111.

28 Bender FA-M, Ramanathan V, Tselioudis G (2012) Changes in extratropical storm track cloudiness 1983--2008: observational support for a poleward shift. Clim Dyn 38(9):2037–2053. Available at: http://dx.doi.org/10.1007/s00382-011-1065-6.

29 Clarke L, et al. (2014) Assessing Transformation Pathways. In: Climate Change 2014: Mitigation of Climate Change. Contribution of Working Group III to the Fifth Assessment Report of the Intergovernmental Panel on Climate Change [Edenhofer, O., R. Pichs-Madruga, Y. Sokona, E. Farahani, S. Kadner, K. Seyboth, A. Adler, I. Baum, S. Brunner, P. Eickemeier, B. Kriemann, J. Savolainen, S. Schlömer, C. von Stechow, T. Zwickel and J.C. Minx (eds.)]. Cambridge University Press, Cambridge, United Kingdom and New York, NY, USA.

30 Xu Y, Zaelke D, Velders GJM, Ramanathan V (2013) The role of HFCs in mitigating 21st century climate change. Atmos Chem Phys 13(12):6083–6089.